Flexural Behavior and Single Fiber-Matrix Bond-Slip Behavior of Macro Fiber Reinforced Fly Ash-Based Geopolymers

Mohammed Farooq[1], Aamer Bhutta[1], Paulo H.R. Borges[2],
Cristina Zanotti[1(✉)], and Nemkumar Banthia[1]

[1] Department of Civil Engineering, University of British Columbia,
6250 Applied Science Lane, Vancouver, BC V6T 1Z4, Canada
{farooq,czanotti,banthia}@civil.ubc.ca,
aamer.bhutta@gmail.com
[2] Department of Civil Engineering, Federal Centre for Technological Education
of Minas Gerais, Belo Horizonte, Brazil
phrbl973@gmail.com

Abstract. A study on flexural response and single fiber-matrix bond-slip behavior in fly ash-based geopolymer reinforced with different types of macro steel fibers is presented. Although direct correlations between bond-slip behavior and composites' flexural response cannot be drawn, investigation of the fiber-matrix bond-slip behavior allows a fundamental understanding of some of the mechanisms involved in the flexural response. Three types of fibers (straight, end-deformed & length deformed), two curing regimes (ambient & heat) under flexural and single fiber pullout conditions are discussed. The performance of geopolymer composites is compared with Portland cement composites. The quantitative effect of fiber geometry is analyzed by introducing the "fiber deformation ratio". End deformed steel fiber exhibits a better performance than straight and length-deformed fibers both in flexural and pullout tests. In the single fiber tests, steel fibers perform better for lower fiber deformation ratios, where the full fiber pull-out mechanism can be exploited; for higher deformation ratios, the strong bearing forces developed, combined with the high adhesion strength of the geopolymer-steel fiber interface, lead to more brittle failure mechanisms, such as fiber breakage or matrix failure. These mechanisms are partially mitigated in the composite (group effect), where end-deformed steel fibers exhibit the most ductile flexural response.

Keywords: Fly ash-based geopolymer · Macro fiber · Steel fiber · Flexural behavior · Deformation ratio · Fiber pullour · Fiber-matrix bond-slip

1 Introduction

The commitment towards limiting the enormous contribution of CO_2 emissions of the cement industry has generated a burgeoning interest in finding alternative binders to OPC (Turner and Collins 2013). Alkali-activated materials (AAM), obtained from the

activation of different agro/industrial by-products (fly ash, slag, rice husk ash, palm oil fuel ash etc.), represent a promising binder alternative.

In light of superior mechanical and durability properties, these materials have attracted increasing interest from the construction sector. Nevertheless, like OPC, AAM classify as quasi-brittle materials, whose crack stability under mechanical loading and severe environmental attacks could be dramatically enhanced through the addition of fiber reinforcement (Shaikh et al. 2013b). Encouraging results are available on the flexural response of fiber reinforced AAM (Shaikh et al. 2013a). Most of the results available, however, are focused on the effect of short or micro steel fibers (< 15 mm length), while little is reported, however, on the behavior of AAM reinforced with macro fibers (>25 mm length) and on the single fiber-mortar bond-slip behavior. The effect of macro-fiber geometry on the single fiber pullout from alkali-activated matrices is discussed by Bhutta et al. (2017). Here, the flexural response of alkali-activated fly-ash reinforced with different types of macro-fibers and possible correlations to the single fiber-mortar bond-slip behavior presented by Bhutta et al. (2017) is discussed. Although no direct correlation can be drawn between flexural response and single fiber behavior, analyzing fiber-mortar bond-slip behavior is an important step towards understanding and optimization of the overall fracture behavior of fiber reinforced alkali-activated composites.
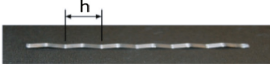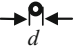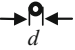
2 Experimental Program

2.1 Materials and Specimen Preparation

Low calcium fly ash conforming to ASTM C615 was activated with an alkaline solution composed of NaOH solution (12 M) and sodium silicate solutions (Na_2O = 14.7%, SiO_2 = 29.4% and water = 55.9% by mass). The resulting matrix, mainly composed of N-A-S-(H) gel, is commonly referred as "geopolymer" (GP), and this term is used hereafter to designate all composites studied. Natural river sand with specific gravity of 2.62 and fineness modulus of 2.83 in saturated surface dry condition was used. Commercially available steel fibers with properties and geometry are shown in Table 1.

Optimum mix proportions based on previous studies (Hardjito et al. 2004; Hussin et al. 2015) consisting sodium silicate (Na_2SiO_3) to 12 molar sodium hydroxide (NaOH) ratio of 2.5 was used. The geopolymers were prepared with an alkaline solution to fly ash ratio of 0.45 by mass and sand to fly ash ratio of 1:1.6. The fiber volume fraction adopted for flexural tests 0.5%. The water to cement ratio of 0.45 by mass and cement to sand ratio of 1:2 were employed for OPC mortars. The fine aggregate and fly ash were dry-mixed for 3 min, after which the alkaline solution was added and mortar was mixed for another 3–5 min while fibers were gradually added. The fresh mortars had a setting time of about 200 min at room temperature, had a stiff consistency and were glossy in appearance. The geopolymers were cast in 100 × 100 × 350 mm prismatic molds for flexural strength test and 75 × 150 mm cylindrical molds for compressive and splitting indirect tensile strength tests. Although due to the high molarity, the workability was relatively low, ample compaction was

Table 1. Properties of steel fibers investigated

Straight		End-deformed fiber		Length-deformed fiber	
	L_f = 50 mm d = 1.0 mm		L_f = 50, h = 6 d = 0.7, b = 1.0		L_f = 50, h =7.5, w = 2.5, t = 0.65
	R_D = 0%		R_D = 6%		R_D = 12%

*L_f =length, d = diameter, w = width, t = thickness, h = single deformed portion (hook) length, b = transverse depth of the deformed portion; **R_D = deformation ratio

achieved with light vibration for 60 s. Single fiber pullout tests were performed using dogbone shaped specimen as described in (Bhutta et al. 2017). All specimens were covered with a plastic film immediately after casting to avoid water evaporation for 24 h. The heat-cured beam specimens were cured at 60°C in an oven for 1-day plus 27 days at room temperature, whereas ambient-cured beams were cured for 28 days at room temperature. OPC specimens were subjected to moist curing (25°C and 95% RH) for 28 days.

2.2   Test Methods

Three replicates for each fiber reinforced geopolymer mortar (FRGPM) were tested in compression, tension, and bending. Compressive strength and splitting tensile strength tests were performed in conformity to ASTM C39 (ASTM C39/C39 M-15a 2015) and ASTM C496 (ASTM C496/C496 M-11 2011) respectively. Third-point flexural tests in accordance with ASTM C1609 (ASTM C1609/C1609 M-12 2012) was performed on the beams using an Instron universal testing machine under closed loop displacement control at a displacement rate of 0.025-0.075 mm/min. The mid-span displacement was recorded as the average of 2 LVDT (Fig. 1-a). The ASTM C1609 parameters discussed in this paper are peak flexural load, flexural toughness, and equivalent flexural strength ratio. Single fiber pull-out tests were performed after 7-day by means of a table mounted test assembly while load and pull-out distances were monitored (Fig. 1-b). Fibre-matrix interfacial bond strength was computed using the Eq. 1.

$$\tau_s = \frac{P_s}{p * l_e} \tag{1}$$

Where τ_s is the interfacial is shear bond stress, P_s is the pullout load at slip s, p is the perimeter and le is the embedded length of the fibre and $l_e = L_f/2$.
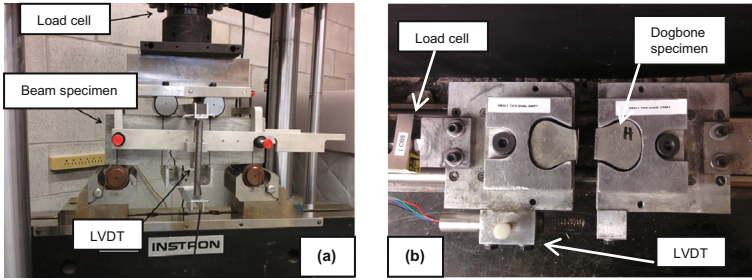
Fig. 1. (a) Flexural test setup (b) Fiber pullout test setup

3 Test Results and Discussion

3.1 Effect of Curing and Fiber Type on Geopolymer Strength

The average compressive and splitting tensile strengths obtained for the GP mortars are shown in Table 2. Compared to ambient curing, mild heat curing provided a significant enhancement of both compressive and split-tensile strengths of the Fiber Reinforced Geopolymer Mortars (FRGPMs). The type of fiber on the other hand, had a much smaller influence on compressive and split-tensile strength as expected.

Table 2. Compressive and Tensile Strengths of FRGPMs

	GP: Ambient (MPa)		GP: Heat (MPa)		OPC (MPa)	
	Comp.	Tensile	Comp.	Tensile	Comp.	Tensile
Straight (S)	22.7	3.6	45.7	5.2	52.3	6.2
End Deformed (ED)	24.3	3.8	48.8	6.1	53.1	6.8
Length Deformed (LD)	23.3	3.8	43.8	5.0	51.6	6.3

3.2 Flexural Response

Average load vs mid-span displacement curves obtained from bending test with third-point loading are shown in Fig. 2. End-deformed steel fibers exhibited the most ductile flexural response, followed, in decreasing order, by straight steel fibers and length-deformed steel fibers. The end-deformed steel fiber was the only type of reinforcement consistently exhibiting deflection-hardening in flexure for all matrices and curing conditions. Length-deformed steel fibers presented a more abrupt post-peak behavior, with softening after the first peak for all specimens. As expected, fibers had a second-order effect on first-peak strength, and similar values were obtained for same matrices cured in same conditions and reinforced with different fibers.

As expected, the type of fibers had the most significant impact on flexural toughness as a result of their ability to bridge cracks, increase the fracture process zone, promote redistribution of localized stresses in the matrix and resist/delay crack
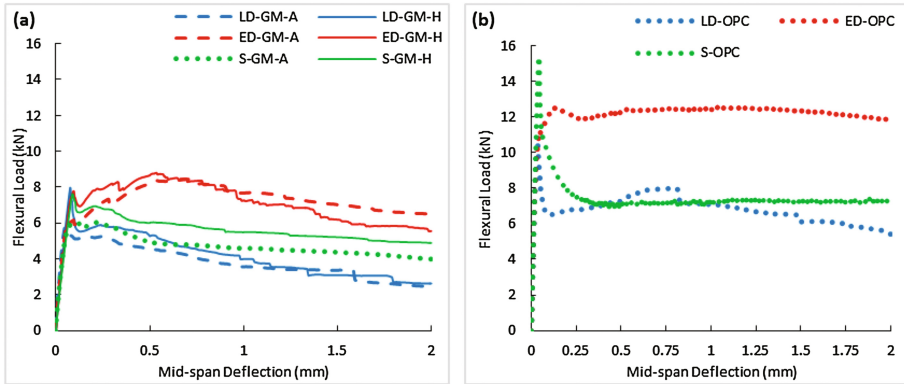
Fig. 2. Flexural Load-deflection curves for different fibers highlighting the effect of (a) curing regime in geopolymers (A = Ambient curing, H = Heat curing) and (b) OPC as reference

propagation. These properties are strongly related to the fiber-matrix bond-slip behavior, affected in turn by the type of fiber and matrix adopted.

The heat curing promoted a marginal improvement in flexural performance of FRGPM; irrespective of the type of fibers, the improvement was smaller than that observed for compressive and tensile tests.

3.3   Single Fiber-Matrix Bond-Slip Behavior

The above mentioned results are in good agreement with fiber-matrix bond-slip behavior for the same geopolymer matrix, curing conditions, and fibers (Fig. 3). The main fiber-matrix slip resisting mechanisms occurring in the fibers investigated here are interfacial adhesions, mainly influenced by chemistry and morphology of the fiber-matrix interface, and matrix-fiber bearing, which is a function of the fiber shape. Once fiber pullout commences, frictional resistance is the significant energy absorbing mechanism. During pullout of deformed fibers, the fiber deforms to take the shape of the groove in the matrix. Therefore, in end-deformed fibers, plastic deformation occurs in the end hook of the fiber, whereas in length-deformed fibers, the mechanism occurs along the whole fiber length.

Steel fibers, as shown in Fig. 3, develop a very strong adhesion with the geopolymer composites compared to OPC. This adhesion is clearly seen to increase when heat curing is employed. This strong adhesion, when combined with high bearing anchorage offered by deformed steel fibers, generates very high fiber-matrix bond strength. The "*deformation ratio*" can be used to quantify the effect of fiber deformation on pullout resistance (Bhutta et al. 2017). In highly deformed fibers, high stresses develop at the fiber-matrix interface while no or little slip occurs. This resulted in fiber fracture in many of the heat cured geopolymer dogbone specimens with end-deformed fibers. The length-deformed fibers, on the other hand, have a larger cross section, thereby comfortably transferred stresses to the matrix. The matrix, however, brittle in nature, underwent progressive fracture prior to or during the pullout. Thus,
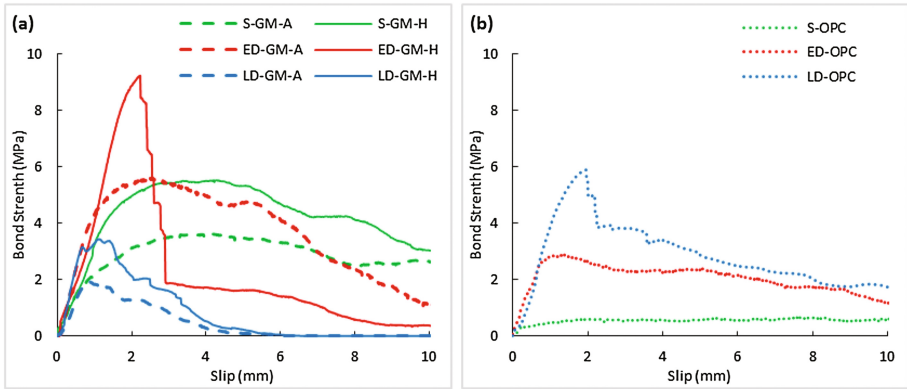
Fig. 3. Single fiber-matrix bond-slip curves for different fibers highlighting the effect of (a) curing regime in geopolymers (A = Ambient curing, H = Heat curing) and (b) OPC as reference

there is a limited capability for stress redistribution. Matrix splitting occurred at higher loads in heat-cured geopolymer specimen. Matrix splitting has been observed in the case of OPC as well (Banthia and Trottier 1994), hence not surprising to see low toughness failure of geopolymers. No matrix splitting was observed in cement composites conducted in this study. Considering the tensile strength of heat cured geopolymer and cement composites was roughly the same, the different failure mode is indicative of the high adhesional bond in geopolymer composites. However, this large adhesional bond was also responsible for the progressive matrix fracture in GP mortars, whereas in OPC mortars, due to a much lower adhesional bond, complete fiber pullout was noted. This In beam specimen, however, the group effect can potentially influence the mechanism of fiber reinforcement, preventing or aiding matrix splitting & fiber fracture, depending on the matrix strength and fiber dosage.

The ideal fiber-matrix bond slip behavior for maximized toughness is one that provides an optimized combination of several factors, including fiber-matrix adhesion and friction, fiber geometry, matrix brittleness, and fiber tensile strength. The most favorable combination of these factors will allow for the following: (i) multiple micro and macro cracking through stress redistribution, so that crack localization is delayed and crack opening is minimized, and (ii) after localization, a gradual pull-out of the fibers bridging the main localized crack so that abrupt fiber rupture is avoided. In this study, the most favorable conditions are achieved with end-deformed steel fibers, offering the highest toughness and followed, in decreasing order, by straight steel fibers, and length-deformed steel fibers.

The flexural response of the FRGPM beams is related to matrix compressive strength and fiber pullout strength in Fig. 4-a and b, respectively. It is generally agreed upon that the first peak of the bending curve typically depends on the properties of the matrix, and fiber reinforcement only has a second order effect. However, one will notice that an increase in compressive (& tensile) strength of heat cured FRGPM compared to the ambient cured specimen does not have any positive impact on the peak
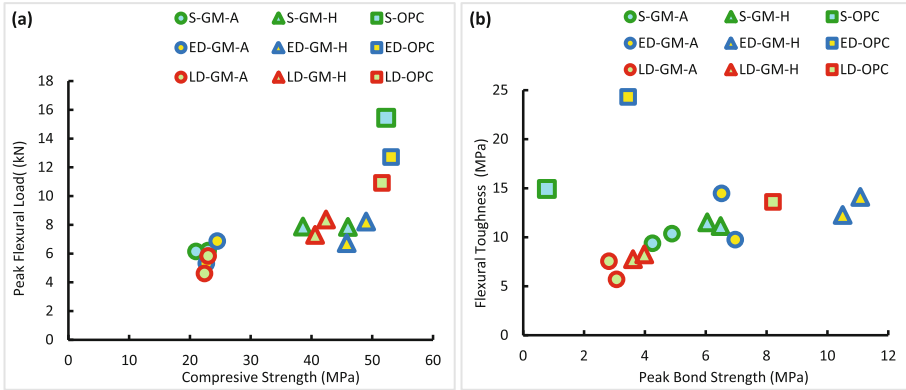
Fig. 4. <u>Effect of</u> (a) compressive strength and (b) single fiber bond strength on flexural properties of fiber reinforced composite beams

flexural strength. The brittle nature of geopolymer matrices with limited micro-crack nucleation in both compression and tension regions of the beam could be the reason for this result.

The fiber type has a significant influence on peak flexural load in case of cement mortar beams (Fig. 4-a). The geopolymer beams, on the other hand, showed practically no change in peak flexural load with different fibers. Irrespective of the fiber type, all geopolymer specimens seem to be following a linear increase in peak flexural load with an increase in compressive strength.

In FRGPMs, a gradual increase in flexural toughness corresponds to an increase in peak bond strength (Fig. 4-b). This increment in flexural toughness is however small, compared to a much larger increase in peak bond strength in heat cured specimens. One can look, for instance, at the behavior of end-deformed fibers, a small increase in flexural toughness is observed despite a significant rise in peak bond strength from ∼6 MPa to over 10 MPa. This is indicative of the importance of additional mechanisms taking place in the beam, including the fiber group effects and the compressive energy absorption component of the flexural beam (Armelin and Banthia 1997). Likewise, between fiber-reinforced OPC mortars and FRGPMs, due to the lower in compressive energy absorption of GP compared to OPC, the full potential of the strong fibre-GP bond is deterred.

The relation between mechanical properties of the FRGPM, single fiber performance and type of fiber are shown in Fig. 5. Figure 5-a highlights the effect of deformation ratio of the fiber on tensile strength & flexural toughness, and Fig. 5-b, the effect of deformation ratio on equivalent flexural strength ratio (ASTM C1609/C1609 M-12) and single fiber bond strength. In all the cases, the end-deformed fibers (6% deformation) provides the best performance.
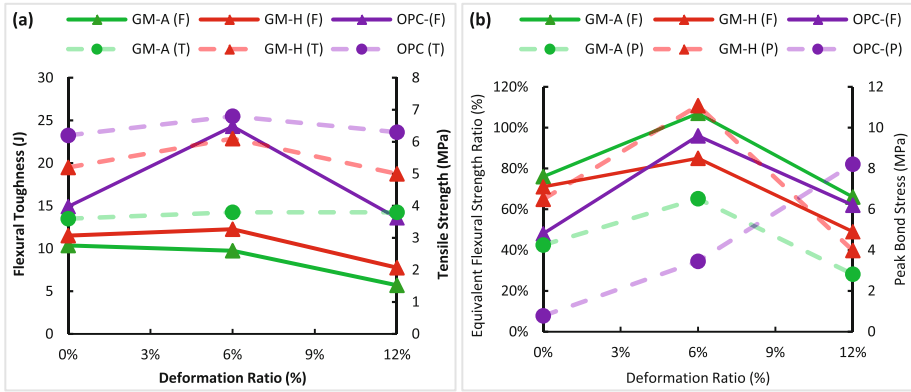
Fig. 5. Effect of fiber deformation ratio on the relation between (a) flexural toughness & tensile strength fiber reinforced composites & (b) equivalent flexural strength ratio & single fiber peak pullout bond strength

4   Conclusions

A study on flexural behavior and single fiber-matrix bond-slip response of geopolymers reinforced with macro-steel-fibers of various shapes is presented. Main conclusions can be summarized as follows:

– Length-deformed fibers are least favorable for the geopolymers analyzed here, due to a large adhesion and bearing anchorage between fiber and matrix, which results in matrix splitting prior to complete fiber pullout;
– End-deformed fibers, on the other hand, depicted the highest values of (peak) bond strength as well as the largest flexural toughness and exhibited, in most occasions, a bending deflection-hardening behavior. In other words, among available shapes, end-deformed fibers are the best to exploit maximized adhesion while providing a ductile fiber-matrix pullout mechanism. This is different from OPC, which, due to the lower chemical adhesion to steel, performs best with larger fiber deformation ratios (length-deformed fibers);
– As expected, a mild heat curing regime significantly increased the geopolymer strength, compared to traditional ambient curing.

References

Armelin, H.S., Banthia, N.: Predicting the flexural postcracking performance of steel fiber reinforced concrete from the pullout of single fibers. ACI Mater. J. **94**(1), 18–31 (1997)

ASTM C1609/C1609 M-12. Standard Test Method for Flexural Performance of Fiber-Reinforced Concrete (Using Beam With Third-Point Loading). ASTM International (2012). doi:10.1520/C1609

ASTM C39/C39 M-15a. Standard Test Method for Compressive Strength of Cylindrical Concrete Specimens **1**, 1–7 (2015). doi:10.1520/C0039

ASTM C496/C496 M-11. Standard Test Method for Splitting Tensile Strength of Cylindrical Concrete Specimen (2011). doi:10.1520/C0496

Banthia, N., Trottier, J.F.: Concrete reinforced with deformed steel fibres. part i: bond-slip mechanisms. ACI Mater. J. **91**(5), 435–446 (1994). doi:10.14359/9765

Bhutta, A., Farooq, M., Zanotti, C., Banthia, N.: Pull-out behavior of different fibers in geopolymer mortars: effects of alkaline solution concentration and curing. Mater. Struct. **50** (1), 80 (2017). doi:10.1617/s11527-016-0889-2

Hardjito, D., Wallah, S.E., Sumajouw, D.M.J., Rangan, B.V.: On the development of fly ash based geopolymer concrete. ACI Mater. J. **101**(6), 467–472 (2004). doi:10.14359/13485

Hussin, M.W., Bhutta, M.A.R., Azreen, M., Ramadhansyah, P.J., Mirza, J.: Performance of blended ash geopolymer concrete at elevated temperatures. Mater. Structures/Materiaux et Constr. **48**(3), 709–720 (2015). doi:10.1617/s11527-014-0251-5

Shaikh, F.U.A.: Deflection hardening behaviour of short fibre reinforced fly ash based geopolymer composites. Mater. Des. **50**, 674–682 (2013a). doi:10.1016/j.matdes.2013.03.063

Shaikh, F.U.A.: Review of mechanical properties of short fibre reinforced geopolymer composites. Constr. Build. Mater. **43**, 37–49 (2013b). doi:10.1016/j.conbuildmat.2013.01.026

Turner, L.K., Collins, F.G.: Carbon Dioxide Equivalent (CO2-E) emissions: a comparison between geopolymer and OPC cement concrete. Constr. Build. Mater. **43**, 125–130 (2013). doi:10.1016/j.conbuildmat.2013.01.023